

Design and Analysis of a High Pressure Ratio Mixed Flow Compressor Stage

Gaurav Giri¹ and Abdul Nassar.²

SoftInWay Turbomachinery Solutions Pvt Ltd. 70/10, Cunningham Road, Bangalore, KA, 560052, India

Dr. Leonid Moroz³, Ivan V Klimov⁴ and Andrey Sherbina⁵

SoftInWay Inc., 1500 District Avenue, Burlington, MA, 01803, USA

Due to higher specific speed compared to conventional centrifugal compressors, mixed flow compressors results in lower frontal area and are hence preferred for small gas turbine engines. With the requirements of higher pressure ratio in mixed flow compressors, the flow at the exit of an impeller is transonic resulting in a complex interaction between the exit flow of impeller and diffuser inlet. Transonic flow in the diffuser, in turn, results in higher diffuser total pressure losses. The design of diffuser for minimizing the pressure loss requires deeper understanding of the flow in the impeller and its interaction with the diffuser. In the present work, a mixed flow compressor stage for a pressure ratio of 5:1 has been designed with isentropic efficiency around 80%. The introduction of diffuser resulted in efficiency degradation. Detailed studies of the flow field give an understanding of the diffuser design. Diffuser geometry has been optimized to improve the overall efficiency of the compressor stage.

Nomenclature

C	= absolute velocity	1	– inlet station
U	= blade speed	2	– outlet station
W	= relative velocity		
P_t	= total pressure		Angle convention:
P_{st}	= static pressure		All angles are defined with respect to tangent
M	= mach number		
B	= flow angle in relative frame		
A	= flow angle in absolute frame		
K	= metal angle		
eff_{tt}	= total to total efficiency		
ptr	= total to total pressure ratio		
z	= number of blades		
C_s	= meridional velocity		
C_p	= pressure recovery coefficient		

¹ Application Engineer, Gaurav.giri@softinway.com.

² Managing Director, abdul.nassar@softinway.com.

³ President and CEO, L.Moroz@SoftInWay.com.

⁴ Application Engineer, ivan.klimov@softinway.com

⁵ Sr. Application Engineer, a.sherbina@softinway.com

I. Introduction

Smaller frontal area and high thrust to weight ratios of mixed flow compressor stage has resulted in its application for small gas turbine engines in aviation sector [1]. The efficiency and reliability of the compressor depends to a great extent on flow behavior in its flow passage and its interaction between impeller and diffuser. The complex turning of the flow not only in the impeller but also in the diagonal diffuser complicates the flow field and requires detailed study of the flow utilizing computational techniques. Stanitz [1952] gave a methodology for the design and analysis of 1-dimensional compressible flow in mixed flow compressors including effects of friction and area change [2]. The size of a compressor can be reduced by adopting the mixed flow compressor without any deterioration of performance.

In the present work, a mixed flow compressor is designed to achieve a total-to-total pressure ratio of 5:1. The compressor's flow path consists of mixed flow impeller, diagonal vaned diffuser, and one more axial vaned diffuser. Design point operation of this compressor is summarized in Table 1.

All iterations of the present study are accomplished utilizing commercial software platform AxSTREAM™ for turbomachinery design, analysis and optimization. Although many loss models exist in the industry, Aungier's loss mechanisms are adopted for mixed flow compressors in the present design study. Loss models for all flowpath components are listed in the Table 2. Various compressor configurations were analyzed to understand the flow field and meet design targets (Table 1).

Table 1 The operating conditions and geometrical constraints of compressor stage

Parameters	Value
Corrected Mass flow rate (kg/sec)	1.74
Stage Pressure Ratio	5.0
Target Isentropic Efficiency stage (%)	79 - 80
Impeller Pressure Ratio	6.2 - 6.5
Target Impeller Efficiency (%)	~90
Rotation speed corrected (rad/sec)	5027
Maximum tip diameter (mm)	260
Maximum axial length (mm)	200

Table 2 Loss models

Flowpath component	Loss model	Deviation model
Mixed flow impeller	Aungier	Wiesner
Diagonal diffuser	Aungier	Howell
Axial diffuser	Lieblein	Lieblein

II. Preliminary Design of the Compressor stage

Based on the available technical specification, using the preliminary design module of AxSTREAM™, the mixed flow compressor stage was designed. To study effects of various parameters and geometry on the performance, the design parameters and geometrical parameters were used in ranges during the preliminary design. Nearly 15000 designs were generated during the preliminary design stage. Different compressor designs were reviewed based on blade metal & flow angles, meridional dimensions, axial lengths, etc. From the preliminary design exploration, it was observed that providing the preswirl at the impeller inlet improves the efficiency by reducing inlet Mach number and losses due to the high velocities at inlet. To turn the flow at the impeller inlet, inlet guide vanes (stationary blade row) are implemented. Figure 1(a) shows the effect of inlet flow angle on efficiency and Figure 1(b) shows the variation of

efficiency with respect to impeller blade exit angle. Figure 1(c) shows the meridional flow path with pressure contours and the 3D geometry of the compressor stage. The final design selected is analyzed further in the meanline/streamline solver.

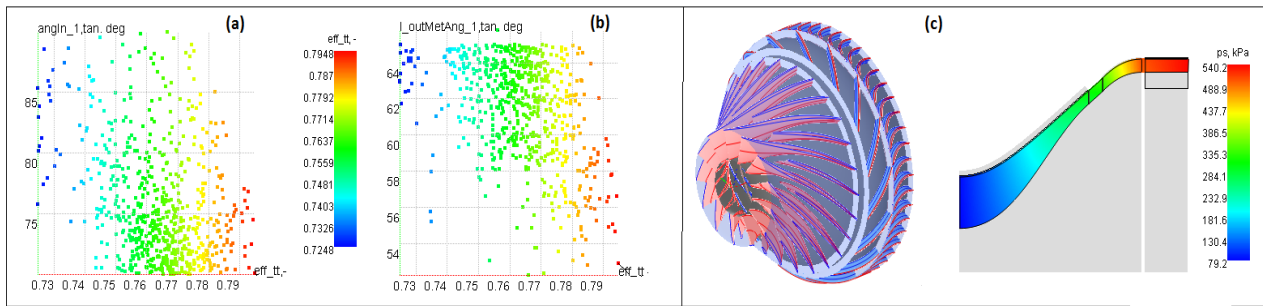


Figure 1. Preliminary Design Explorer (a) efficiency vs. inlet flow angle; (b) efficiency vs. impeller exit blade angle; (c) 3D compressor view & meridional view with static pressure contour

III. Detailed compressor design

A. Description of Solvers

Four different solvers were utilized in the current design: meanline, streamline, full streamline solver (FSC), and axisymmetric CFD. Meanline solver calculates kinematic and thermodynamic parameters accounting for real losses listed in Table 2. At this level, important aerodynamic criteria and experience help the designer to evaluate designs. Streamline analysis was performed adding additional conservation equations to the compressor analysis. Streamline analysis accounts for radial non-uniformity in thermodynamics, kinematics, and losses. FSC solves the compressor in meridional plane and qualitatively shows averaged velocity distribution. End-wall contours were profiled based on FSC results on a quasi-orthogonal grid. The axisymmetric CFD analysis was performed to understand the flow behavior and to compare the results with the meanline and streamline results. The losses at the hub, mean and tip sections were reviewed during each iterations of the design to achieve minimum losses in the impeller. At first, it was observed that the overall stage performance was not satisfactory and significant losses exist in the diffuser. An initial off-design analysis showed the operational margin was also not in the desired range. Hence, the authors decided to optimize the impeller first and then tackle the diffuser problems to obtain the required performance.

B. Impeller Optimization

End-wall contours are optimized to ensure the smooth flow through the impeller. Subsequently, the distribution of BETA & THETA are modified to increase the throat value and also to increase the total to total pressure ratio generated by the impeller. Initially a splitter with length ratio of 0.7 was used and subsequently the splitter was extended to 0.8 which resulted into better pressure ratio and operating margins. Figure 2(a) shows the slope of the impeller inlet and Figure 2(b) shows the slope angle at the impeller exit which was optimized to reduce the losses in the vaneless space as it leaves the impeller.

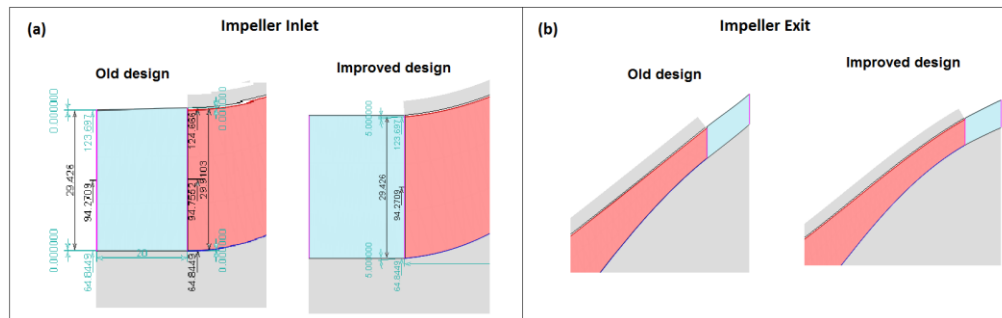


Figure 2. Editing of impeller geometry at inlet/outlet station

Figure 3(a) shows the quasi-orthogonal grid that is generated for the full streamline solver (FSC). Figure 3(b) shows the contours of Mach number for the impeller in the meridional plane for the initial impeller and the optimized impeller using full streamline (FSC) solver. To validate the FSC solver results, both impellers were also calculated using axisymmetric CFD solver and the Mach number contours for initial and optimized impeller design were presented in Figure 4 which are having good qualitative agreement with the FSC solver results.

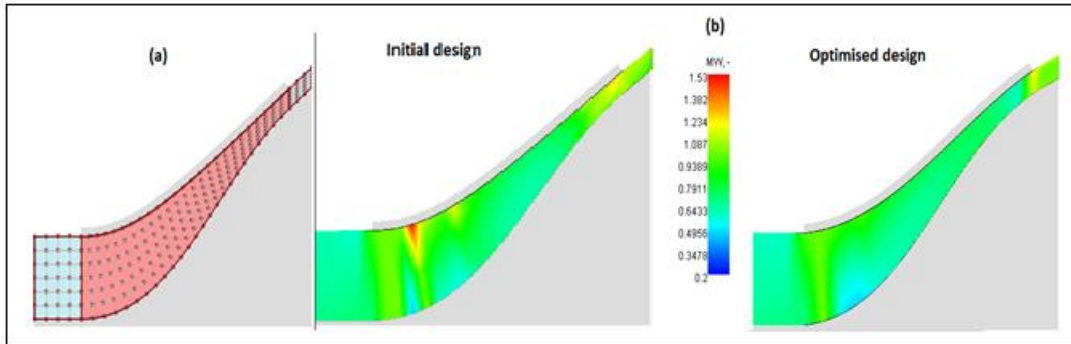


Figure 3. Contours of Mach number of the initial and optimized flow path using FSC solver

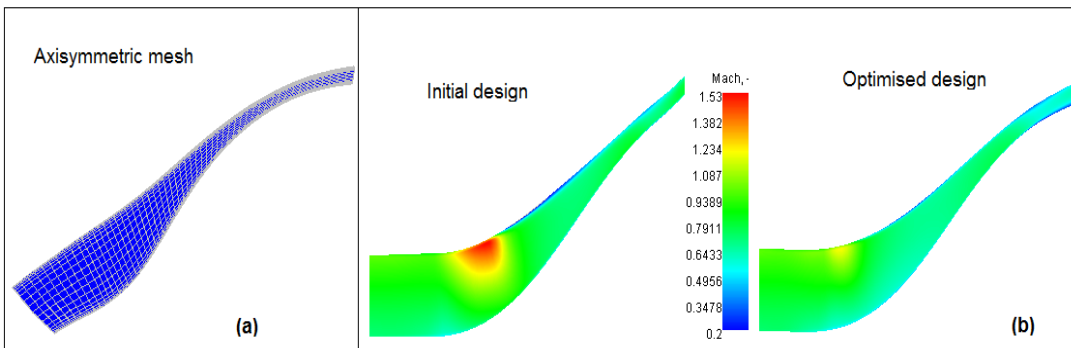


Figure 4. a) axisymmetric mesh; b) axisymmetric CFD solution -- Mach number contours

The performance of the impeller at both design and off-design operation was calculated for the initial impeller and for the final impeller. The results are presented in Figure 5. Charts show that not only there is improvement in efficiency but also the improvement in pressure ratio and operational range. The final compressor characteristic shifted to the right which resulted in establishing sufficient choke margin comparing to the earlier design.

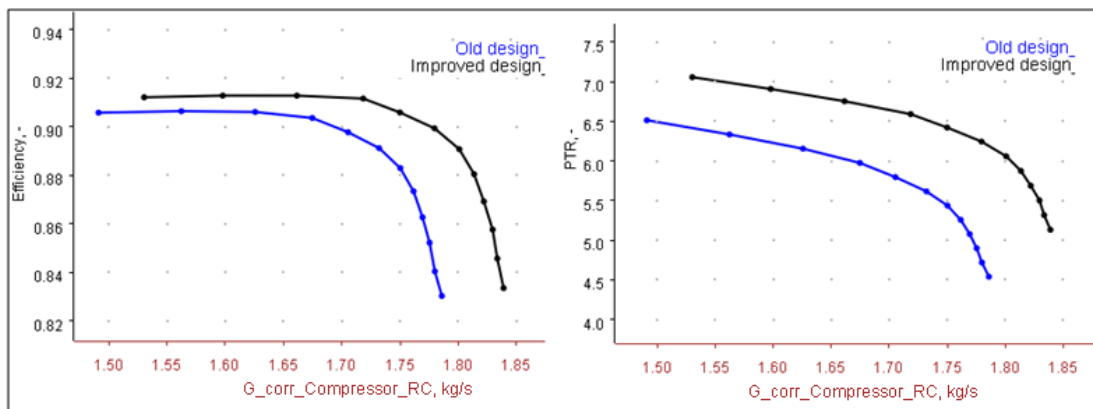


Figure 5. Comparison of old design and improved design after editing of impeller

To analyze the flow structure and also to obtain the performance map in 3D CFD, full RANS based CFD analysis was performed in CFD module of the AxSTREAM™. Profiling was done prior to CFD analysis and Figure 6(a) shows

the distribution of the BETA, THETA and thickness at the mean section of the impeller. Red, blue and green color curves represent the BETA, THETA and thickness distribution, respectively. The angle values represented in Figure 6(a) are with respect to meridional plane. Figure 6(b) shows the 3D view of the blade profile for both splitter and main blade. 3D CFD analysis of the final impeller geometry is compared with the streamline calculation results in Figure 7. The choke mass flow difference between streamline solver and CFD is about 1.35% whereas the efficiency at design point differed by about 1.2% when compared between the streamline solver and CFD solver. Streamline and 3D performance predictions show good agreement.

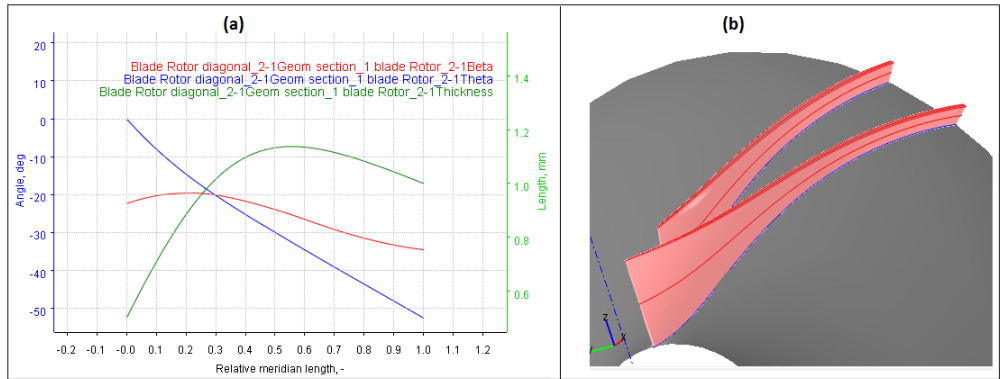


Figure 6. (a) THETA, BETA & Thickness distribution for impeller (b) 3D view of the profile

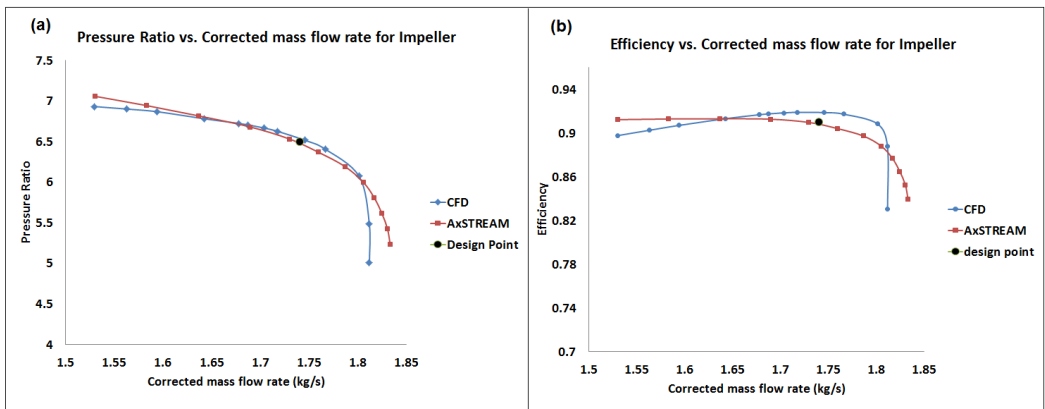


Figure 7. Impeller performance: a) pressure ratio (total-total) versus corrected mass flow rate; b) efficiency versus corrected mass flow rate

The blade loading distribution at hub, mean and tip section for the main blade and splitter blade is show in Figure 8. The local static pressure is normalized with inlet total pressure. The loading looks smooth and within norm.

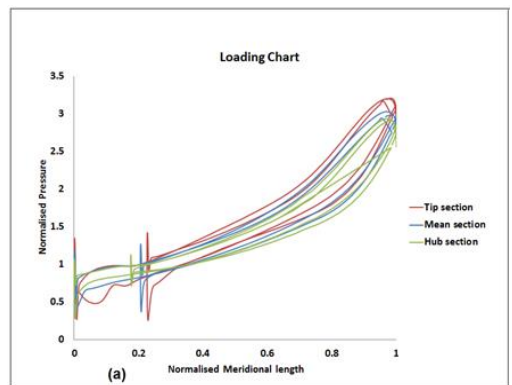


Figure 8. Blade loading

As the next step, diffuser was introduced for the optimized impeller and performance was calculated using the streamline solver. It was observed that the losses in diffuser were significantly high resulting in lower performance of the stage.

C. Diagonal Diffuser optimization

The major constraint on the diagonal diffuser was the maximal tip diameter. The flow at the exit of impeller was transonic and this resulted in shock formation at the diffuser inlet. 3D CFD analysis was performed to understand the flow interaction between the impeller, vaneless space and diffuser. Figure 9, shows the various configurations of diffusers studied during this phase. It was observed that total pressure loss in initial diffuser was very high. Initial diffuser design has 20% total pressure loss and the modified diffuser pressure loss is 8%. The losses were reduced by optimizing the inlet and outlet angle of the diffuser, varying the axial length of the diffuser, the channel height ratio at the inlet and outlet, and the profile.

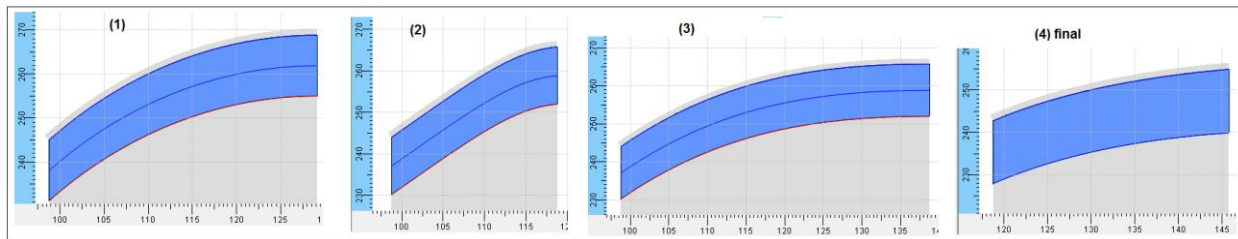


Figure 9. Diagonal diffuser shapes

While calculating the stage with initial diagonal diffuser, some blockage at design point was noticed in the streamline results and later verified with CFD results. In streamline solver, losses due to blockage and flow separation can be predicted by the *separated flow mix loss factor* [3], om_{mix} , which was equal to 0.00033 at design point and increases in the direction of stall condition which reduces the stage stall margin. CFD calculation was performed for the point slightly left to the design point and analysis showed the huge blockage in the diagonal diffuser passage. The reason was improper diffuser profile. To overcome this, profile of the diffuser was edited using BETA & THETA distribution of the diffuser vane and *separated flow mix loss factor* [3] dropped to 0.00021. Figure 10 shows the diffuser geometry. While making the adjustments in the profile, throat area was reduced which resulted in diagonal diffuser passage additional choking losses. Such type of choke losses of the components can be predicted by the *choke loss factor* [3], om_{ch} , in AxSTREAM. To avoid the choke losses at the design point, number of diffuser vanes was reduced from 14 to 12 along with the blade thickness. The number of diffuser vanes can be reduced even further and implement diffuser splitter vanes to control the choke loss and to provide the better flow turning in the diffuser passage. The desired performance was achieved with the optimized diffuser and the author did not implement diffuser splitter vanes.

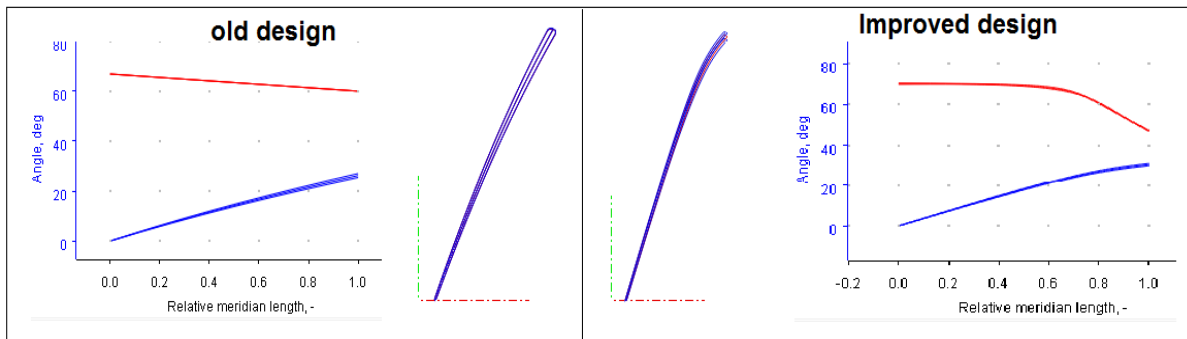


Figure 10. Diagonal diffuser profile, BETA, and THETA curves

Since the required velocity was not achieved at the exit of the vaned diffuser, an additional axial stator was introduced at the exit of diagonal diffuser vane. DCA profiling was used for the axial stator blades with the main objective of reducing the swirl at the exit and recovering the static pressure to maximum with minimal losses in the stage.

Figure 11 shows the flow path contour of the final compressor stage consisting of impeller, diffuser and the axial stator and also the 3D view of the compressor stage.

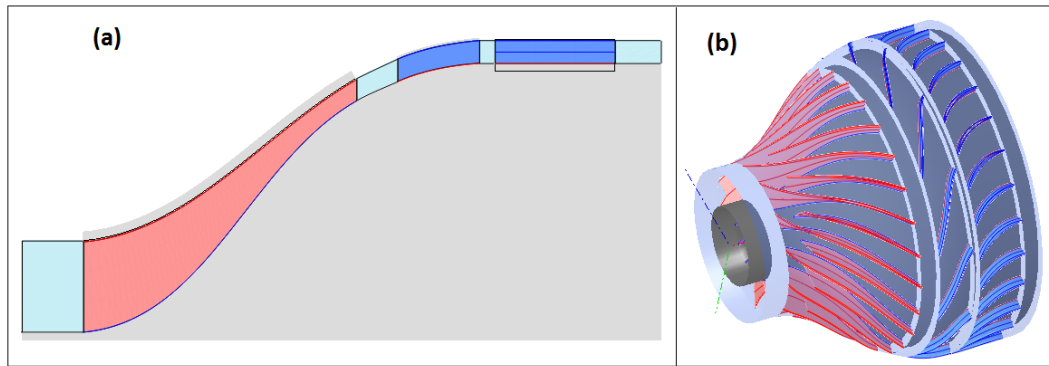


Figure 11. Compressor final design: a) meridional view; b) 3D view

Figure 12 shows the kinematics on the mean section of each flow path component for the designed compressor stage. The stage performance parameters and geometry of the designed compressor are listed in Table 3 and Table 4, respectively.

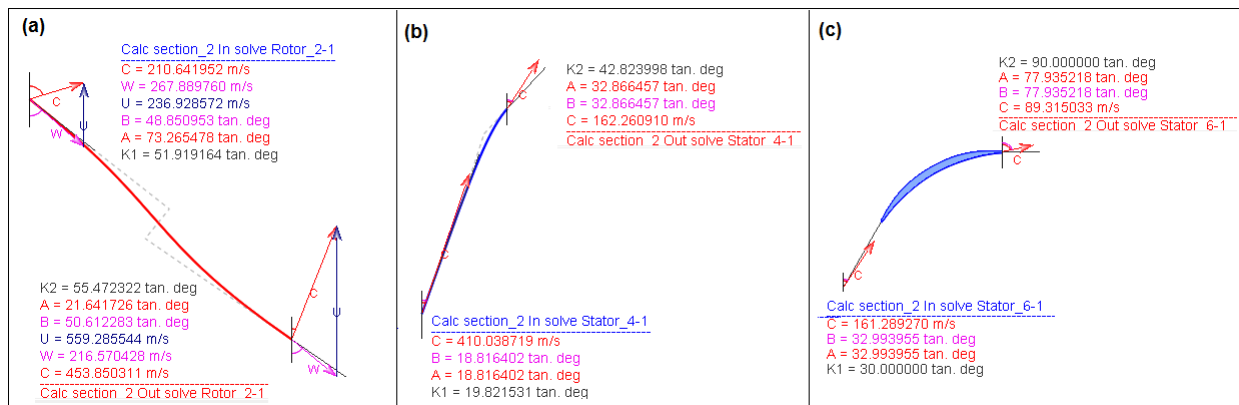


Figure 12. Stage kinematics

Table 3 Stage characteristics

Sl. No	Parameter	Unit	Value
1	Mass flow rate at inlet	kg/s	1.74
2	power	kW	391
3	Isentropic efficiency	%	79.1
4	Polytropic efficiency	%	83.27
5	total-total pressure ratio	-	5.2
6	Inlet flow angle	deg	73
7	Specific speed	-	0.48
8	Equivalent diffusion factor [3]	-	1.54
9	Flow coefficient ($C2s/U2$)	-	0.29
10	Work coefficient (specific work/ $U2^2$)	-	0.70
11	Diagonal diffuser, C_p	-	0.6521
12	Axial diffuser, C_p	-	0.319

Table 4 Geometric parameters of the final stage

Parameter	value	Parameter	value
Impeller tip diameter ratio	0.54	Diag. diff. exit tip diameter	255mm
Impeller hub diameter ratio	0.301	Diag. diff. axial length	30mm
Number of impeller vanes	26 (13+13)	No. of diag. diff. vanes	12
Impeler exit blade angle	55.5deg	Exit blade angle of diag. diff.	43deg
Tip clearance	0.3 mm	No. of axial diff. vanes	28
Hub-to-tip diameter ratio at impeller inlet	0.52	Exit blade angle of axial diff.	90deg
Blade height ratio (inlet to exit)	4.25	Axial length of axial diff.	39mm
Axial length of impeller	89mm	Compressor axial length (without IGV)	172

D. Off-design Performance

Initially, the off-design performance was analyzed for one speed line. Detailed off-design performance for various speed lines are presented in Figure 13 which was performed using the AxMAP module based on the streamline solver. Figure 13(a) shows total-to-total pressure ratio versus corrected mass flow and Figure 13(b) presents isentropic efficiency versus corrected mass flow rate for speeds of 100%, 95%, 90% and 85% of the corrected design speed 5027 rad/sec.

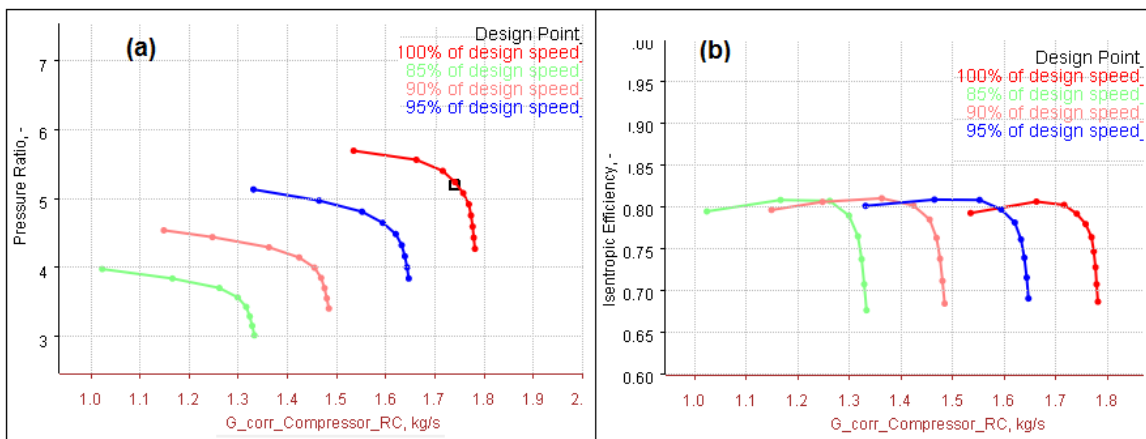


Figure 13 Streamline off-design performance prediction: (a) pressure ratio vs. corrected mass flow rate; (b) efficiency vs. corrected mass flow rate

IV. 3D CFD and results

AxSTREAM™ provides sufficient tools to take design from 1D-meanline to 3D CFD with intermediate steps at streamline, FSC solver, and axisymmetric CFD. To reduce the overall time required between design iterations, a simplified and fast approach is used where FSC is used in most of the cases instead of performing a full scope 3D CFD analysis for the entire domain. In some cases, axisymmetric CFD analysis provided some insights on the flow structure. Figure 14 shows the comparison of the contours of total pressure performed in meanline solver, FSC, and 3D CFD. The results agree qualitatively.

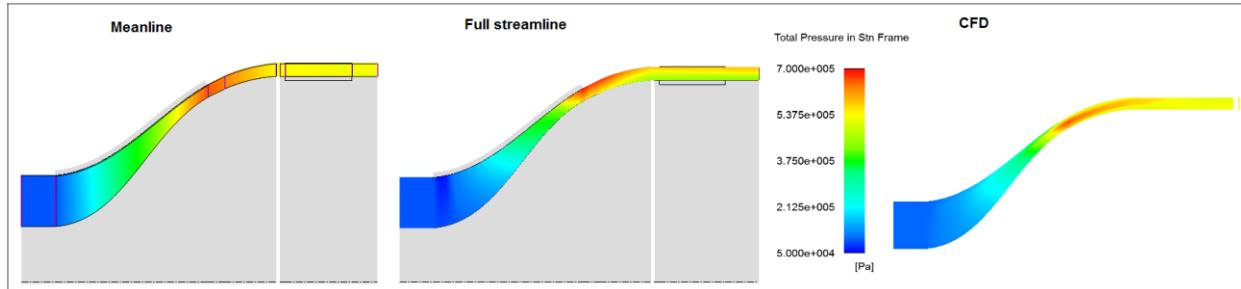


Figure 14. Total Pressure Contour using meanline solver, FSC solver & 3D CFD

The results of detailed 3D CFD analysis within the AxSTREAM™ platform are discussed in this section. The mesh was generated in AxCFD module using the automated mesh generation technique with user defined factors in terms of the boundary layer and mesh density. Figure 15 shows the computational fluid domain for the compressor stage and also the meshed domain highlighting the critical areas where fine mesh was required. “K-epsilon” turbulence model was used with the convergence criteria of 10^{-6} . After the solution convergence, the mass imbalance was checked and found to be less than 0.001%.

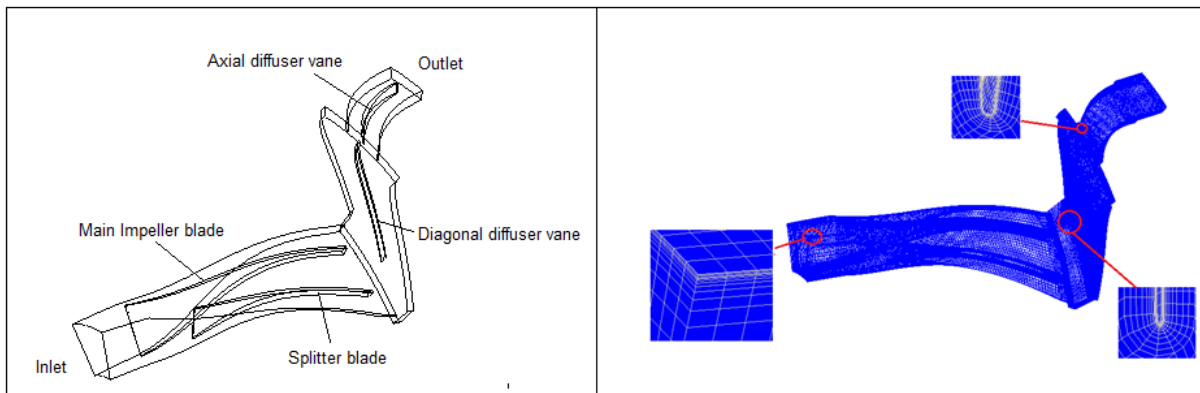


Figure 15. Flow Domain of the compressor stage

3D CFD analysis was performed not only for the design point but also for off-design operation to determine the stall and choke flow. CFD results are compared with results from streamline solver which was used to design this compressor stage. Figure 16 shows the performance map calculated by both streamline and CFD solvers on the design speedline – and results are in good agreement. Streamline solver predicts 2.3% higher pressure ratio at the design mass flow and near stall point, the maximum difference in predicted pressure ratios is about 4.9%. Streamline solver under-predicted the performance in terms of efficiency and the difference in design point is about 1.55%. When compared with the impeller alone performance, the stage choke mass flow has reduced by about 3%. The stall margin for the stage has changed by about 2% compared with the impeller alone performance. This shows that introduction of downstream components has resulted in reduction in operation margins by about 2 – 3 % at both extremes of the operating range.

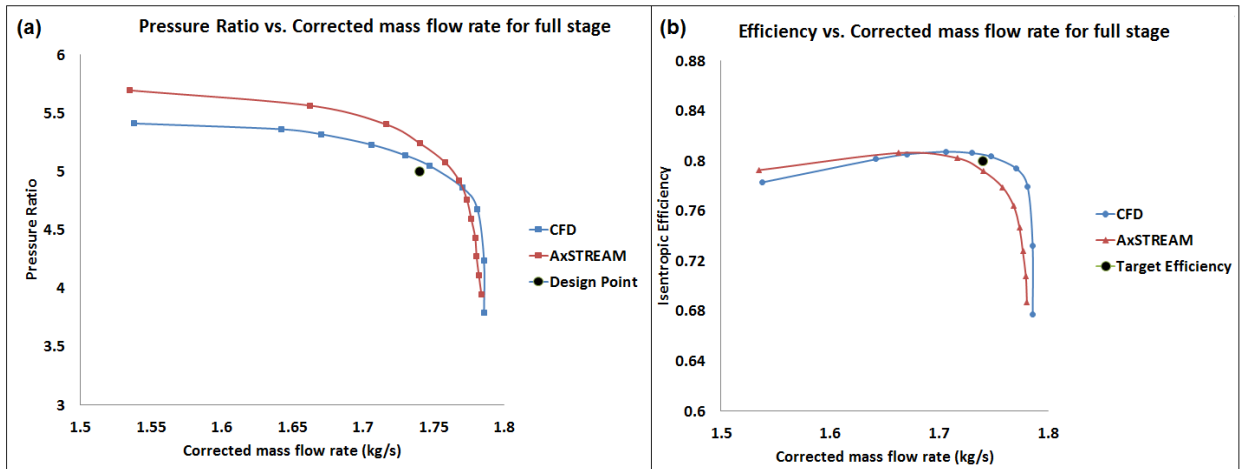


Figure 16. Stage performance: a) pressure ratio & b) isentropic efficiency vs. corrected mass flow rate

The meridional projection of Mach number contours, meridional velocity and pressure is presented in Figure 17. From the relative Mach number contour plots, it was noticed that maximum relative Mach number is greater than one at the tip of the impeller inlet. Then, relative Mach number decreases from inlet to impeller exit. The flow at the impeller exit is supersonic and some additional losses are present in the vaned diffuser due to shock formation.

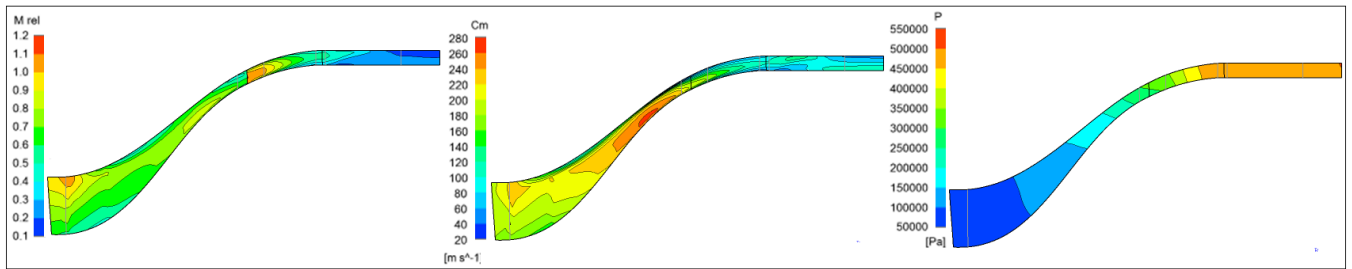


Figure 17. Mach number, meridional velocity & pressure contours

The critical area to be studied is the region between the impeller and the diffuser. Detailed flow analysis was performed by obtaining the Mach number contours and total pressure at different stations (1 through 24) shown on meridional view in Figure 18.

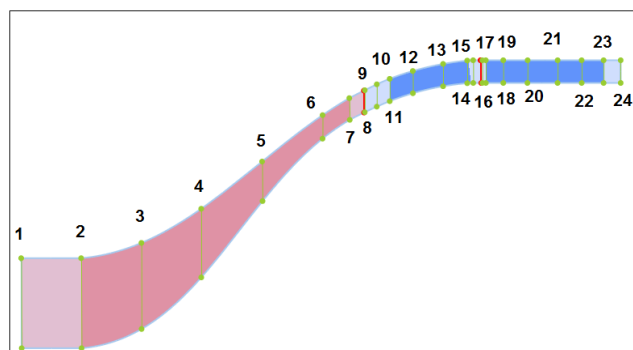


Figure 18. Plane location

Figure 19 shows the relative Mach number contours at station planes from the inlet to the exit of the stage (see Figure 18). Plane 1 through plane 8 show the relative Mach number contours for impeller, plane 9 through 16 covered the Mach number variation in diagonal diffuser passage, and plane 17 through 24 covered the Mach number variation in axial diffuser passage. For impeller passage, plane 2 shows the Mach number variation at the impeller leading edge

and it has been noticed that Mach number at the tip is greater than 1. As the flow passes the impeller passage, relative Mach number decreases and has lower value near the tip region. For diagonal diffuser passage, plane 9 shows the transonic flow regime. As flow transitions towards the vaned diffuser inlet, it decelerates. As it approached the leading edge of the diffuser at plane 11, high Mach number was observed locally at the suction side of the diffuser which is due to the local acceleration of the flow at the leading edge of the diffuser. As the flow passed the leading edge (planes 12, 13, 14), diffusion takes place recovering some static pressure.

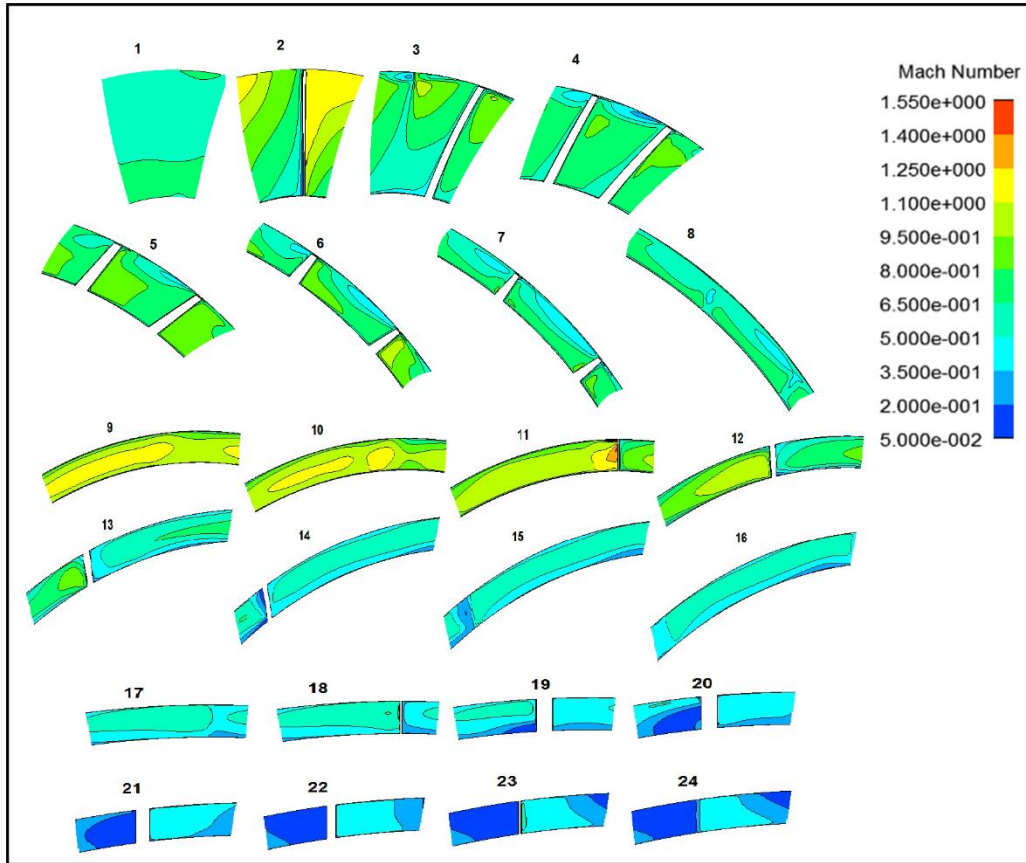


Figure 19. Mach number distribution for full stage

Axial diffuser was used to provide the flow turning and to recover the residual energy to static pressure. As from the plane 17 to 24, it is noticed that flow velocity gradually reduces and at the suction side of the diffuser blade flow separation begins at the 50% of the streamwise blade length near the blade tip. Because velocity of the flow at the inlet of axial diffuser is not high, the total pressure loss is not high in the axial diffuser passage.

Figure 20 depicts the total pressure (in stationary frame) contours for the full stage at different stations shown in Figure 18. Plane 1 through 8 shows the total pressure variation in the impeller passage. Total pressure increases gradually from plane 1 to 4. From plane 5 to 8, some of the total pressure loss occurs near the tip region due to the tip clearance. Plane 9 to 16 shows the total pressure variation in diagonal diffuser passage and the loss of total pressure is noticed in the contours. Plane 17 to 24 shows the total pressure variation in axial diffuser passage and some of the total pressure loss occurred in the axial diffuser passage. Because velocity is not very high, pressure loss is small comparing to pressure loss in diagonal diffuser.

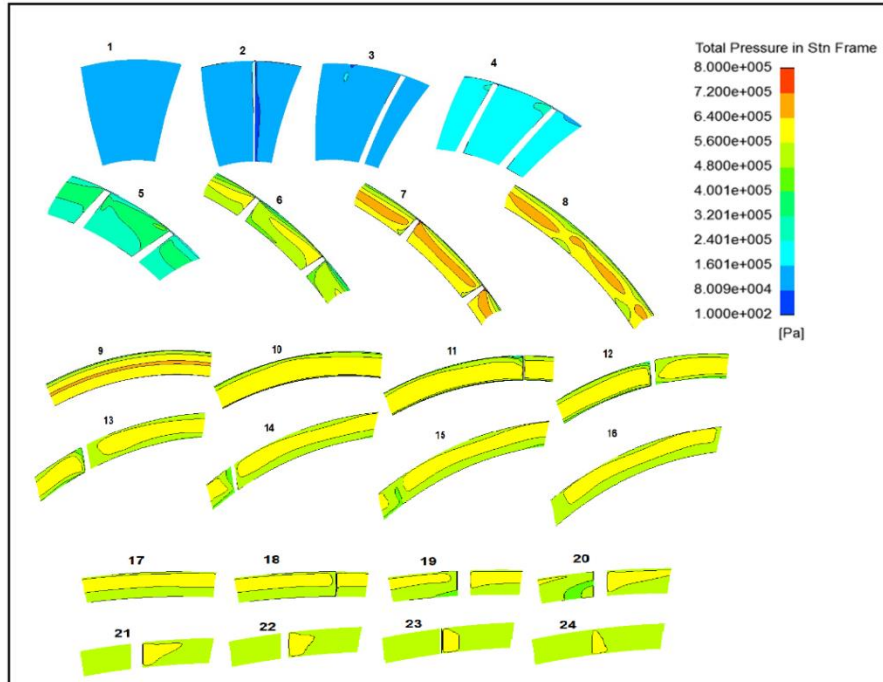


Figure 20. Total Pressure distribution for full stage

V. Conclusion

- A mixed flow compressor with a pressure ratio of 5.2:1 was designed utilizing software platform AxSTREAM™. Integrated approach from preliminary design to 3D CFD analysis results in considerable time reduction in design practices.
- In a high pressure ratio mixed flow compressor, flow at the impeller exit is supersonic and the change in flow direction to axial in the diffuser results in significant diffuser losses.
- A detailed analysis of the flow field interaction between the impeller and diffuser is necessary to minimize the losses and improve the overall performance of the compressor.
- Based on streamline and 3D CFD analyses, one might conclude that the final design of high pressure ratio mixed flow compressor stage in the current study satisfies the objective and performance requirements: pressure ratio, efficiency, the maximum tip diameter and maximum axial length. This clearly demonstrates the successful utilization of 1D- and 2D-solvers for designing similar compressor stages.

References

- ¹Ramesh Rajakumar, D., Govardhan, M., and Ramamurthy, S., "CFD analysis of flow through mixed flow compressor under various operating conditions," International Journal of Scientific & Engineering Research, Volume 4, Issue 2, February 2013, ISSN 2229-5518
- ²John D. Stanitz, 1952. "One Dimensional compressible flow in Vaneless Diffusers of radial and Mixed-flow centrifugal compressors including Effects of friction heat transfer and area change." NACA TN 2610. Lewis Flight Propulsion Laboratory, Cleveland, Ohio
- ³Aungier, Ronald H., 2000, "Centrifugal Compressors: a strategy for aerodynamic design and analysis, ISBN 0-7918-0093-8